

STUDY OF PLASMA-EDGE TURBULENCE REDUCTION IN NEGATIVE TRIANGULARITY PLASMAS USING THERMAL HELIUM BEAM DIAGNOSTIC IN THE TCV TOKAMAK

M. UGOLETTI

ISTP-CNR, Institute for Plasma Science and Technology, corso Stati Uniti 4 – 35127 Padova, Italy
Email: margherita.ugoletti@istp.cnr.it

M. AGOSTINI, M. LA MATINA

Consorzio RFX (CNR, ENEA, INFN, UNIPD, Acciaierie Venete SpA) Corso Stati Uniti 4, 35127 Padova, Italy

Y. WANG, C. THEILER, O. KRUTKIN, M. BONISSOLLI, O. SAUTER, S. CODA, O. FEVRIER, B. LABIT
EPFL, Swiss Plasma Center (SPC), CH-1015, Lausanne, Switzerland

S. RIENÄCKER, P. HENNEQUIN

Laboratoire de Physique des Plasmas (LPP), CNRS, Sorbonne Université, Ecole polytechnique, Institut Polytechnique de Paris, Palaiseau, France

TCV TEAM

See author list of B.P. Duval et al 2024 Nucl. Fusion **64** 112023

WPTE TEAM

See the author list of E. Joffrin et al 2024 Nucl. Fusion **64** 112019

Abstract

A thorough understanding of the plasma edge is crucial for improving both confinement and stability in fusion reactors. Several strategies are currently being investigated to mitigate edge turbulence and minimize its impact on transport. Recent studies suggest that negative triangularity (NT) plasmas may offer significant advantages over conventional positive triangularity (PT) configurations. These include enhanced confinement, reduction of core turbulence-driven transport, and the elimination of edge-localized modes (ELMs), which are known to cause significant stress on reactor walls. As a result, NT is increasingly being considered a promising alternative for next-generation fusion devices. This contribution presents recent experimental results obtained using the upgraded Thermal Helium Beam (THB) diagnostic on the TCV tokamak. A key focus of the study is the influence of plasma geometry on edge profiles and fluctuations, particularly in relation to turbulence suppression mechanisms. Special attention is given to the differences observed between PT and NT plasmas. The analysis highlights the substantial reduction in edge turbulence observed in NT configurations, reinforcing the potential benefits of this shaping approach for improved confinement. New insights are obtained thanks to the fact that THB diagnostic can measure kinetic profiles and fluctuations across the last closed flux surface.

1. INTRODUCTION

For the realization of future fusion reactors, it is essential to optimize plasma control in order to prevent disruptive events that may damage reactor components, and to ensure stable and long-term operation. A major challenge in this, regards the control of edge-localized modes (ELMs), which can release large, transient heat fluxes onto plasma-facing components, potentially compromising their integrity [1]. To mitigate or suppress these events, several strategies have been proposed, ranging from active control techniques to alternative plasma shaping. Among the latter, negative triangularity (NT) configurations have recently attracted increasing attention. Plasma shaping indeed is one of the key tools for optimizing confinement and stability in tokamaks. Among the shaping parameters, triangularity has a particularly strong impact on turbulent transport and magneto-hydrodynamic (MHD) stability [2]. While conventional reactor scenarios have traditionally focused on positive triangularity, recent theoretical and experimental studies have demonstrated that NT plasmas can exhibit improved core energy confinement, reduced turbulence-driven transport, and access to high-performance regimes without type-I ELMs, even at moderate plasma current and magnetic field [3].

Considering that, a deep understanding of the plasma edge features is fundamental for enhancing plasma confinement and stability in future fusion reactors. A valuable diagnostics for characterizing the edge plasma is the Thermal Helium Beam (THB). This diagnostic has gained increasing significance due to its capability to simultaneously measure edge electron temperature T_e and density n_e profiles, along with their fluctuations. The THB system relies on the measurement of selected helium spectral line emissions, which, using Collisional-Radiative models, provide crucial information about plasma parameters with high spatial and temporal resolution.

The original THB diagnostic from the RFX-RFX-mod experiment has been upgraded and recently installed at the outer mid-plane of the Tokamak à Configuration Variable (TCV). This optimized diagnostic will be mounted in the RFX-mod2 experiment, thanks to EU funding for the NEFERTARI project, under the Italian National Recovery and Resilience Plan (NRRP). The Tokamak à Configuration Variable (TCV), located at the Swiss Plasma Center in Switzerland, is a medium-sized tokamak with a conventional aspect ratio. It has a major radius of $R = 0.88$ m and a minor radius of $a = 0.25$ m, housed within a highly elongated vacuum vessel equipped with a versatile divertor system [4]. TCV is equipped with 16 independently powered poloidal field coils, providing exceptional plasma shaping flexibility, enabling operation with elongations up to $\kappa \approx 2.8$ and triangularities in the range $-0.7 < \delta < 1$. In recent years, significant efforts have been dedicated to enhancing the diagnostic suite on TCV, particularly for investigations of the plasma edge and scrape-off layer (SOL). The study of fluctuation-driven particle and heat transport requires diagnostics capable of resolving the temporal evolution of key plasma parameters - such as density and electric fields - with high spatial and temporal resolution. Moreover, it has been demonstrated that correlating density fluctuations with fluctuations in the radial phase velocity provides a reliable method to estimate $E \times B$ turbulence-driven transport in the plasma edge region [5].

These findings allow the possibility to investigate the statistical properties of turbulent transport in the core region of fusion plasmas based on measurements of density fluctuations. During last years, the THB was used to measure a wide range of pulses in NT, exploring different plasma configurations, triangularity, and elongation. In this contribution, a dataset of discharges in NT together with their PT counterparts is analyzed, performing a statistical study of the edge plasma properties in terms of density and temperature profiles as well as turbulence characteristics. Subsequently, two identical discharges, except for the triangularity opposite to the X-point, are compared. By examining the effects of plasma shaping on edge transport properties, this work contributes to the ongoing efforts to optimize plasma performance in fusion reactors.

2. DIAGNOSTIC DESCRIPTION

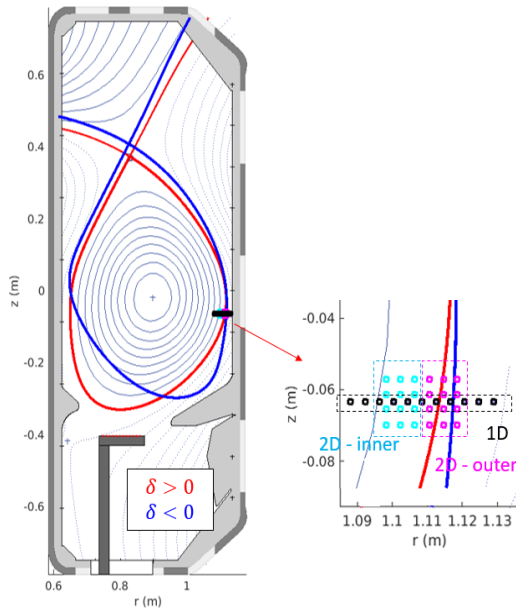


FIG. 1 TCV tokamak poloidal cross section with PT and NT equilibria studied in this contribution. A zoom on the outer mid-plane plasma-edge region observed by the THB, indicating the 2 possible configurations (one 1D and two 2D) is also shown.

The Thermal Helium Beam (THB) is a plasma edge/scrape off layer diagnostic used for simultaneously measuring the electron temperature (T_e) and density (n_e) profiles, as well as their fluctuations. It has already been used in most of the fusion plasma experiments: RFX-mod [6], JET [7], ASDEX Upgrade [8], Wendelstein 7-X [9] and TCV [10]. It exploits the line ratio technique for estimating n_e and T_e in the edge and divertor region of fusion plasmas, measuring three visible HeI lines: 667.8 nm, 706.5 nm and 728.1 nm. This set of lines is selected considering their typical emissivity when a small amount of He is puffed in the plasma, without perturbing it, and the diverse temperature and density responses exhibited by singlet-singlet and singlet-triplet line intensity ratios. To reconstruct the values of n_e and T_e , the experimentally measured ratios of selected lines are compared with a collisional radiative model (CRM) [11]. One of the main limitations of this technique is related to the fact that the two-line ratio technique does not consider the effect of the radiation trapping of ultraviolet resonance line, leading to an overestimation of n_e and T_e . One way to take into account this effect is by measuring a fourth HeI line, at 501.6 nm, adding a third line ratio, which is mainly proportional to photon re-absorption [12][13]. The new THB measuring 4 HeI lines, so to include a direct estimate of the photon re-absorption, is developed for RFX-mod2 experiment and it is currently in use to characterize the plasma edge at the mid-plane of TCV experiment [10]. The

THB has been installed at the external mid-plane of TCV in 2022, sharing the port-hole and puffing system of the existing Gas Puffing Imaging diagnostics [14] (see Fig. 1). It is composed of eight channels connected to eight of the twelve available lines-of-sights with 4 mm diameter, connected to MPCC detectors, capable of resolving plasma fluctuations up to 500 kHz [6]. The diagnostic provides excellent results across the separatrix region, specifically for ρ values between 0.96 and 1.08, with a spatial resolution of 4 mm (diameter of the line-of-sight). The eight lines of sight are usually arranged horizontally in a one-dimensional (1D) configuration, providing a radial coverage of about 4 cm around the separatrix, from the plasma edge to the SOL. In June 2025, a second

fibre bundle with a 4x3 configuration was installed, enabling two-dimensional measurements of smaller plasma regions. Its positioning can be chosen by rotating the bundle by 180°, allowing measurements either closer to the plasma edge or further into the SOL. A representation of the diagnostic location in the TCV plasma cross-section and the different line-of-sight setups, is shown in Fig. 1. The TCV equilibria plotted correspond to the NT (in blue) and PT (in red) configurations that will be mostly analysed in the following. One of the main strengths of this diagnostic is its ability to simultaneously measure n_e and T_e profiles, as well as their fluctuations, even though the experimental limitations associated with studying these two quantities are different. To reconstruct n_e and T_e profiles, it is necessary to utilize all four emission lines. One of these lines in particular – the 728 nm – is included in all three ratios but is typically very weak, thus setting the experimental limit on the temporal resolution at which such profiles can be determined. Moreover, the amount of helium that can be puffed into the plasma is constrained by the requirement not to perturb the plasma itself. At TCV it operates effectively in a density range between 1×10^{18} and $5 \times 10^{19} \text{ m}^{-3}$, with temperatures ranging from few eV up to a maximum of 170-200 eV. Depending on the signal level, T_e and n_e profiles can be evaluated with a time resolution as low as 1 ms. To study plasma edge turbulences, instead, the temporal evolution of a single line – the brightest one – can be used. In this way, plasma edge turbulences can be investigated with a temporal resolution of 100-500 kHz, enabling the characterization of plasma behaviour even during high turbulence events, such as ELMs [15]. The amount of radiation emitted by a spectral line in the plasma is in fact associated with a radiative transition from neutral atom state p to state q . It depends on the neutral density and the local n_e and T_e and it can be written as $S_{pq} = n_0 f_p(n_e, T_e) A_{pq}$, where n_0 is the ground state neutral density, the function $f_p(n_e, T_e)$ is the ratio of the density of state p to the ground state density, and A_{pq} is the radiative decay rate of the p to q transition. The local n_0 is determined by the local He gas puff, which is constant over the turbulence timescale ($\sim 1 - 10 \mu\text{s}$) and slowly varying over the turbulence space scale ($\sim 2 - 10 \text{ cm}$). Thus, the local light emission rate should follow, as a first approximation, the local changes in density and temperature due to fluctuations in the frequency range of interest. The line used in this work is primarily the 667 nm, which is the brightest one and its intensity is mainly proportional to electron density.

3. OVERVIEW OF TURBULENCE DEPENDENCE ON NT

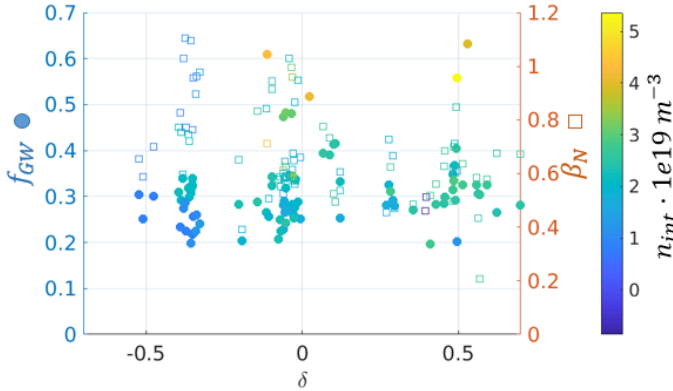


FIG. 2 $f_{GW} = n_e/n_{GW}$ – solid circles, β_N (empty squares) and integrated density n_{int} (color-map) as a function of delta of the selected subset of discharges.

One of the goals of this work is to apply this plasma edge diagnostic for the first time to study the TCV plasma in the outer mid-plane, focusing on the role of the triangularity. During 2024–2025, a wide range of scenarios in NT – together with their counterpart in PT – were explored, during which measurements with THB were performed. All the data considered were collected in L-mode. The explored experimental pulses are summarized in Fig. 2, in terms of $f_{GW} = n_e/n_{GW}$ (solid circles), β_N (empty squares) and n_{int} (colour-map). On the x-axis, the total plasma triangularity. As expected, the confinement enhancement is observed – increase in β_N – as the triangularity is decreased, for almost the same interval of values of f_{GW} and n_{int} explored. Before specifically comparing identical pulses in NT and PT, some statistical analysis was carried out on the collected data. For this purpose, the set of data was separated into two subsets, based on the triangularity δ values: $\delta < -0.1$ in blue and $\delta > 0.1$ in red. In Fig. 3 - a), the average radial profiles of plasma pressure of these two subsets, measured by the THB, are shown. From the comparison between the two regimes, it is evident that the values of p_e measured in NT are higher both in the SOL and in the plasma edge, with respect to those in PT. From the analysis of the values

of n_e and T_e , separately, it can be discerned that both n_e and T_e profiles are higher, as already observed in many plasmas [16][17], as well as in TCV [18][19]. Another observed behaviour in NT plasmas is a reduction of the edge turbulence [20]. This quantity can also be evaluated using the THB diagnostic. From the same dataset, the fluctuation level of the signal corresponding to

the brightest emission line is analysed. This represents the most straightforward approach to assess the amplitude of fluctuations.

A common way to quantify this is through the ratio of the standard deviation, σ , to the mean value, μ , of the measured emissivity. To first order, this ratio provides an estimate of the relative fluctuation level detected by the diagnostic. The evolution of σ/μ as a function of ρ for the same subsets is shown in Fig. 3 - b). While inside the separatrix the difference between the two regimes is minimal, being slightly higher in NT, it becomes more pronounced and inverted when moving towards the SOL. On average, outside the separatrix the turbulence level is lower in NT than in PT, consistent with Refs. [21]. It should be noted that in these plots, the turbulence level is averaged over a large database of diverse shapes and regimes, further confirming the overall reduction of plasma transport in NT plasmas. Another important quantity used to study plasma turbulence is the probability density function (PDF) of the transported quantities, in this case of the emissivity which in turn is proportional to plasma density. In plasma turbulence, the PDF describes the likelihood of different values occurring over time, rather than focusing on average values. PDFs reveal non-Gaussian, often exponential or extreme value distribution tales, indicating the prevalence of strong, coherent structures and bursty, non-uniform transport. Skewness and kurtosis are employed to characterize the shape of the PDF. Skewness quantifies the asymmetry of the distribution, with positive values indicating a prevalence of large positive fluctuations. Kurtosis, instead, measures the degree of intermittency, with values exceeding 3 pointing to intense, localized events in plasma turbulence. The skewness and the kurtosis of the two subgroups, PT and NT, are shown in Fig.3 - c) and d), respectively. For both quantities, the PT plasma shows higher values as one move away from the separatrix towards the SOL, confirming the hypothesis of a reduction of turbulence in NT in this plasma region. This higher level of skewness can be related to the presence of coherent plasma structures with higher density – and temperature – than their surroundings, in the form of filamentary structures, also known as blobs. They represent a substantial fraction of radial heat and particle transport, and they play a key role in setting the tokamak SOL profiles [22] and the level of plasma interaction with the first wall [23]. For these reasons a good understanding of the physics governing their cross-field motion

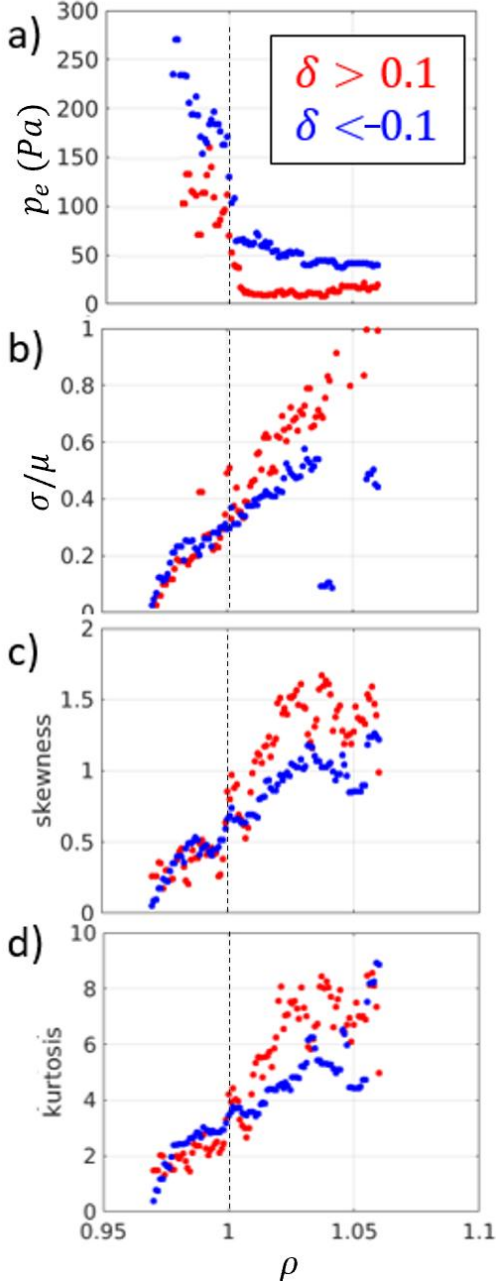


FIG. 3 Comparison PT vs NT of plasma pressure (a), σ/μ (b), skewness (c) and kurtosis (d) as a function of ρ for the set of pulses shown in Fig. 2.

is of great importance. For this purposes, two discharges in PT and NT are examined in detail, to characterize the structural differences between these two plasma configurations. The comprehensive radial and two-dimensional coverage of the THB, combined with its capability to resolve both fluctuations and the absolute values of n_e and T_e , is exploited to enable a more in-depth analysis.

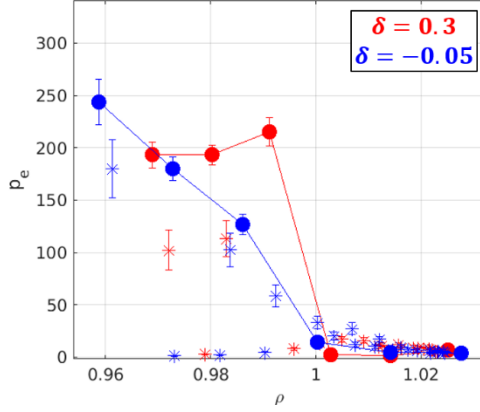


Fig. 4 Plasma pressure profiles measured by the THB (solid circles) and TS (asterisk) in PT (red) and NT (blue) plasmas

these two shots, it is possible to evaluate the frequency spectrum, which is shown in Fig. 5– a) for three different radial positions. The red profiles always represent the PT data (#83051), while the blue ones correspond to NT (#83052). The analysis is performed using the calibrated brilliance of the brightest line. The power spectrum of plasma edge turbulence quantifies how the energy of turbulent fluctuations is distributed across different frequencies and wavelengths. The PSD can typically be divided into three distinct regions, which are clearly evident in the PT profiles and, just inside the separatrix, in the NT ones. The *high frequency region* (f^{-n} , with $n \geq 2$), associated with small-scale events involving localized portions of the system. The *low frequency region* (approximately f^0), corresponding to global-scale isolated events. The *intermediate region* (f^{-1} scaling), indicative of overlapping avalanche-like transport. In NT plasma, the PSD tends to exhibit a more pronounced f^{-1} behaviour as the separatrix is approached and into the SOL, while the high-frequency, steep-slope component characteristic of the turbulent regime is largely absent. This behaviour can be discussed related to the other quantity shown here, i.e. the autocorrelation function ACF in Fig. 5 – b).

This provides an estimate of how long turbulent eddies remain temporally correlated. The autocorrelation analysis reveals systematic differences between the two regimes (PT vs. NT curves). Outside the separatrix, the red curves exhibit a faster decay of autocorrelation and, at the separatrix, stronger oscillatory behaviour. This indicates a shorter memory of the velocity fluctuations and therefore a higher level of turbulence. Conversely, the blue curves decay more slowly and remain positive over longer time scales, reflecting more coherent structures, as observed by the PSD. These results indicate that, by reversing the triangularity, the role of long-range dependence in the flow shear region is enhanced, while the radial propagation of avalanches contributes to a stronger self-similar character of the fluctuations in the SOL [26].

While so far, the turbulence analysis has treated the individual THB LoS as independent, a cross-correlation analysis allows for a more complete picture of the structures in this region. To study that, the Conditional Average (CA) technique is applied to the signal measured by all the THB LoSs. Conditional averaging (CA) is a data analysis technique used in plasma physics to study the turbulent edge by revealing the characteristics of intermittent, turbulent events that would otherwise average out with simple statistical methods. By defining a trigger condition, such as the occurrence of a specific fluctuation or event, a time series can be conditionally

4. COMPARISON BETWEEN PT AND NT PULSES

The two selected plasma shapes are those shown in red (PT) and blue (NT) in Fig. 1. They are chosen because the USN configuration provides the best match with other plasma turbulence diagnostics, namely Doppler Backscattering DBS [24] and Short Pulse Reflectometry [25], with which a comparison will be presented in future work. These two discharges are identical except for the triangularity opposite to the X-point, which has been reversed. In Fig. 4, the pressure profiles are compared. The asterisks represent the measurements obtained from Thomson Scattering. It can be observed that the two diagnostics reconstruct the edge plasma profiles in a very similar way, with THB slightly overestimating the pressure in PT. As previously noted, the pressure profile in NT is more peaked, with a steeper gradient. To study the fluctuation level in

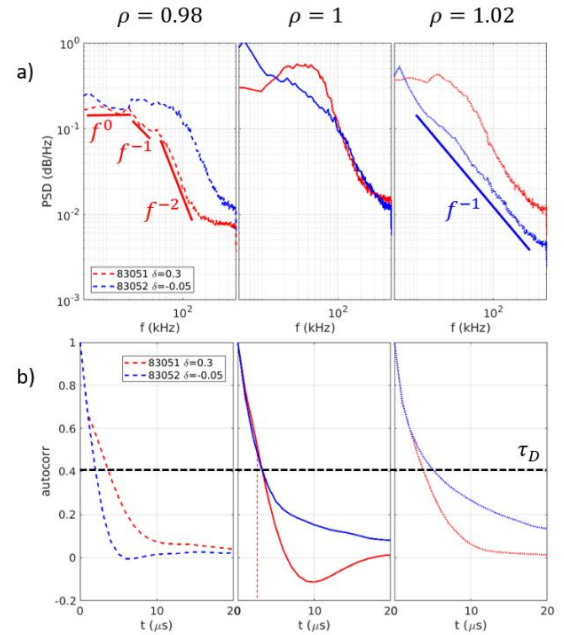


Fig. 5 a) PSDs and autocorrelation b) measured by THB at three different radial positions

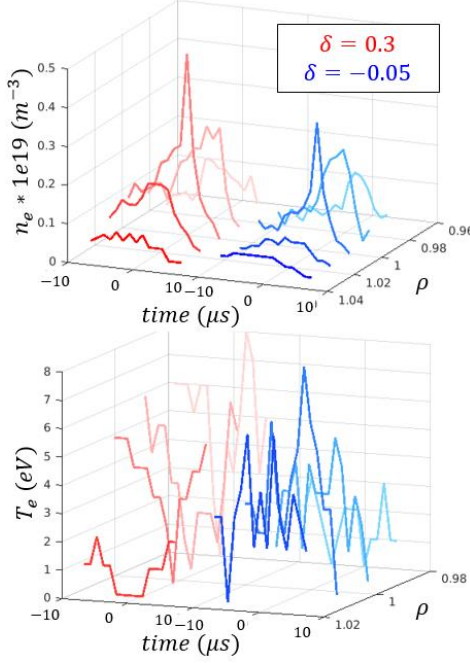


Fig. 6 n_e at the top, T_e at the bottom at 4 radial positions calculated with the CA technique. The peaks used to select the blobs are the ones measured by the LoS at $\rho = 1$.

systematically higher in the PT regime compared to NT, the temperature measured outside the separatrix is comparable to that observed in PT. From the analysis of these results, preliminary inferences can be drawn regarding the temporal extension of the blobs and their propagation velocity. To better compare the different sizes of the blobs measured in these two regimes, the normalized CA n_e profiles are shown in Fig. 7, for two radial positions. In all the compared LoSs, the blob width measured in PT is larger than that in NT. The size of the blob is estimated as the average value, i.e. $11 \mu\text{s}$ in PT and $5.6 \mu\text{s}$ in NT. In both regimes, the blobs become wider going towards the SOL. By analysing the time delay of conditionally averaged signals in adjacent lines of sight, instead, one can infer the radial projection of the blob velocity. It should be noted that blobs tend to be strongly elongated along the poloidal direction, and that in the region observed by THB their radial velocity is typically one order of magnitude lower than their poloidal velocity [27][28]. Given that, the estimated velocity can be regarded as a combination of both, predominantly governed by the poloidal component. The estimated velocities are $v_{PT} = 2.15 \text{ km/s}$ in PT plasma, $v_{NT} = 4.3 \text{ km/s}$. These velocities are consistent with those estimated by DBS in two discharges nearly identical to those discussed in this work, as reported in Ref. [29]. This agreement suggests that the estimation obtained with THB provides a reliable approximation of the blob poloidal propagation velocity, both in terms of absolute value and in its variation. From this analysis results than PT has more, slower and larger blobs, while NT has less, faster and narrower blobs, consistent with previous measurements and simulations [21]. To perform a more detailed study of blob velocities, the 2D setup was employed. Due to the limited number of available channels (8 channels), the 2D coverage is restricted to a relatively small spatial region. Nevertheless, this approach allows a more accurate investigation of the blob propagation direction, including its density and temperature variations. Preliminary results are shown in Figure 8.

averaged to form a representative structure. This process helps filter out random noise and extract meaningful information about the dynamics, such as the spatial and temporal behaviour of structures like blobs and holes in turbulence, their lifetimes, and propagation speeds. For the analysis shown below, the trigger is defined using the 667 nm-signal measured on the separatrix. The peaks are defined as the values that exceed $[\mu + 1.6\sigma]$ threshold. Once these peaks are identified on this LoS, the average of the brilliance in the time interval $[\pm 20 \mu\text{s}]$ around each peak is calculated, at the same time instants for the 8 LoSs and the four wavelengths. The innovative aspect of this work lies in computing the CA across all wavelengths, which enables the application of the CR model to evaluate the density and temperature of the identified blobs. In Fig. 6, the n_e time evolution is shown at the top, and T_e at the bottom, for 4 selected lines of sight around $\rho = 1$. The CA analysis was performed over a 70 ms time window. During this interval, the number of blobs identified in the NT plasma is 35% lower compared to that measured in the PT plasma (720 vs 1100). The blobs appear mainly as variations in density, while they do not have a clear structure in T_e . It can be observed that, along the line of sight where CA was calculated, i.e. at $\rho = 1$, an anticorrelation in temperature is apparent in the PT data, while it is not evident in the NT case. At the same time, although the blob density remains

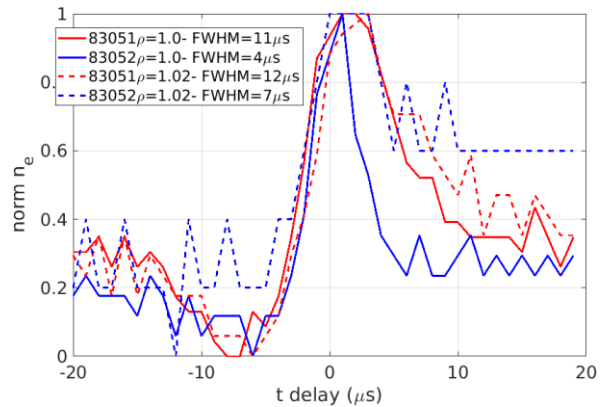


Fig. 7 Comparison of the normalized blob density for three positions shown in Fig. 6 in PT and NT.

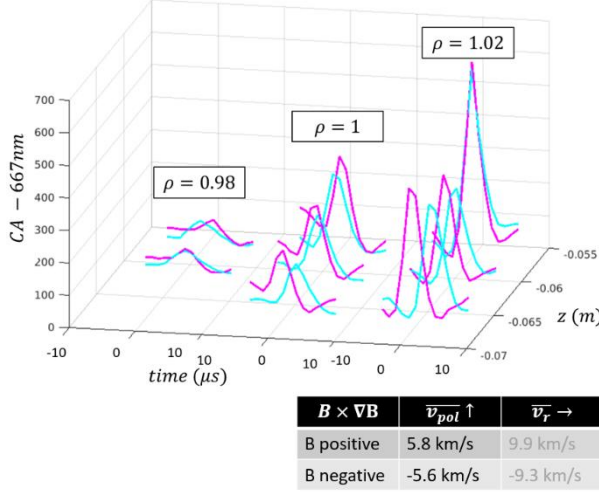


Fig. 8 CA of the 667nm line with the 2D THB configuration in two NT pulses with opposite $B \times \nabla B$

The CA was calculated along the outermost line of sight ($\rho = 1.02$, $z = -0.55\text{m}$). The simplest way to verify whether the measured velocity is mainly poloidal or radial is to reverse the toroidal magnetic field. This reversal leads to an inversion of the $\nabla p \times B$ direction drift outside the separatrix, whereas the radial component is expected to remain unchanged. From the analysis of the time delay between the CA peaks in these two discharges, the velocities reported in the table in Fig. 8 are obtained. Since the measured radial velocity is higher than the poloidal velocity and changes sign when the magnetic field is reversed, we conclude that the velocity measured by the diagnostics is dominated by the poloidal component, as previously observed in the 1D analysis. To achieve more accurate measurements of blob evolution, either additional channels are required, or dedicated scans should be

performed in which the plasma position is varied.

5. CONCLUSIONS

In this work, results obtained with the THB diagnostic have been presented. For the first time, a large dataset of discharges, covering different plasma shapes and opposite triangularities, has been analysed using shape alone as the discriminant. In addition to a generalized study of edge plasma properties, a more detailed comparison has been carried out between two otherwise identical discharges with opposite triangularity. The THB diagnostic has been employed to investigate both density and temperature profiles as a function of plasma shape, as well as to characterize turbulent fluctuations. All results confirm previous observations from other devices and from numerical simulations. In particular, it has been highlighted that, despite the broad differences among the discharges, common features can be identified between the two configurations: a higher plasma pressure with steeper gradients, a reduction of temperature towards the SOL, and a decrease of turbulent activity as quantified by the skewness and kurtosis of the PDFs in NT with respect to PT plasmas. Once this statistical trend was established, a more detailed analysis of two discharges, differing only in the sign of *non - Xpoint* δ , was carried out. Consistent with previous evidence of its predominant role in turbulence reduction, both PSDs and autocorrelation functions showed a decrease in turbulence intensity from the separatrix to the SOL. THB measurements were further used to study the shape, velocity and propagation direction of blobs identified through conditional averaging. This method revealed that blobs appear primarily as density perturbations, which are both more intense and broader in PT than in NT, with no corresponding structure observed in temperature. These turbulent structures were then studied by comparing 1D and 2D results. Altogether, the analysis has confirmed the capability of this diagnostic to characterize the plasma edge region. The collected data have validated trends already observed in other studies, showing a reduction of turbulence levels when moving to negative triangularity. Thanks to the high temporal resolution of the diagnostic, future work will focus on extending this analysis to high-performance plasmas, with the aim of studying edge characteristics as profiles approach H-mode transitions also in NT, thereby shedding further light on the physics governing turbulence in these regimes.

ACKNOWLEDGEMENTS

This work has been carried out within the framework of Italian National Recovery and Resilience Plan (NRRP), funded by the European Union—NextGenerationEU (CUP B53C22003070006, ‘NEFERTARI’). Views and opinions expressed are however those of the author(s) only and do not necessarily reflect those of the European Union or the European Commission. Neither the European Union nor the European Commission can be held responsible for them. This work has been carried out also within the framework of the EUROfusion Consortium, partially funded by the European Union via the Euratom Research and Training Programme (Grant Agreement No 101052200 - EUROfusion). The Swiss contribution to this work has been funded by the Swiss State Secretariat

for Education, Research and Innovation (SERI). Views and opinions expressed are however those of the author(s) only and do not necessarily reflect those of the European Union, the European Commission or SERI. Neither the European Union nor the European Commission nor SERI can be held responsible for them. This work was supported in part by the Swiss National Science Foundation.

REFERENCES

- [1] J. P. GUNN et al., Surface heat loads on the ITER divertor vertical targets, *Nucl. Fusion* **57** 046025 (2017).
- [2] A. O. NELSON et al., Prospects for H-mode inhibition in negative triangularity tokamak reactor plasmas, *Nucl. Fusion* **62** 096020 (2022).
- [3] A. MARINONI et al., A brief history of negative triangularity tokamak plasmas, *Reviews of Modern Plasma Physics* (2021).
- [4] B. P. DUVAL et al., Experimental research on the TCV tokamak, *Nucl. Fusion* **64** 112023 (2024).
- [5] C. HIDALGO et al., Fluctuations, sheared radial electric fields and transport interplay in fusion plasmas, *New J. Phys.* **4** 51 (2002).
- [6] M. AGOSTINI et al., Fast Thermal Helium Beam diagnostic for measurements of edge electron profiles and fluctuations, *Rev. of Scient. Instrum.* **86**, 123513 (2015).
- [7] S. J. DAVIES et al., Parallel electron temperature and density gradients measured in the JET MkI divertor using thermal helium beams, *Journal of Nuclear Materials*, **241–243**, 0022-3115 (1997).
- [8] M. GRIENER et al., Helium line ratio spectroscopy for high spatiotemporal resolution plasma edge profile measurements at ASDEX Upgrade, *Rev. of Scient. Instrum.* **89**, 10D102 (2018).
- [9] T. BARBUI et al., The He/Ne beam diagnostic for line-ratio spectroscopy in the island divertor of Wendelstein 7-X, *JINST* **14**(07) C07014 (2019).
- [10] M. UGOLETTI et al., Role of radiation re-absorption in the thermal helium beam diagnostic, *Rev. of Scient. Instrum.* **95**, 083530 (2024).
- [11] M. GOTO, Collisional-radiative model for neutral helium in plasma revisited, *Journal of Quantitative Spectroscopy and Radiative Transfer* **76**, Issues 3–4 (2003).
- [12] S. KAJITA et al., Helium line emission spectroscopy in recombining detached plasmas, *Physics of Plasmas* **25**, 063303 (2018).
- [13] S. KAJITA et al., Comparison of He I line intensity ratio method and electrostatic probe for electron density and temperature measurements in NAGDIS-II, *Physics of Plasmas* **13**, 013301 (2006).
- [14] N. OFFEDDU et al., Gas puff imaging on the TCV tokamak, *Rev Sci Instrum.* **93** (12) 123504 (2022).
- [15] M. LA MATINA et al., Experimental characterization of inter-ELM modes in type-I ELM scenarios at TCV using the thermal helium beam diagnostic, *Plasma Phys. Control. Fusion* **67** 085034 (2025).
- [16] A. MARINONI et al., H-mode grade confinement in L-mode edge plasmas at negative triangularity on DIII-D, *Phys. Plasmas* **26**, 042515 (2019).
- [17] A. MARINONI et al., Diverted negative triangularity plasmas on DIII-D: the benefit of high confinement without the liability of an edge pedestal, *Nucl. Fusion* **61** 116010 (2021).
- [18] Z. HUANG et al., Dependence of density fluctuations on shape and collisionality in positive- and negative-triangularity tokamak plasmas, *Plasma Phys. Control. Fusion* **61** 014021 (6pp) (2019).
- [19] S. CODA et al., Enhanced confinement in diverted negative-triangularity L-mode plasmas in TCV, *Plasma Phys. Control. Fusion* **64** 014004 (2022).
- [20] W. HAN et al., Suppression of first-wall interaction in negative triangularity plasmas on TCV, *Nucl. Fusion* **61** 034003 (2021).
- [21] K. LIM et al., Effect of triangularity on plasma turbulence and the SOL-width scaling in L-mode diverted tokamak configurations, *Plasma Phys. Control. Fusion* **65** 085006 (2023).
- [22] D. A. D'IPPOLITO et al., Convective transport by intermittent blob-filaments: Comparison of theory and experiment. *Physics of Plasmas*, **18**(6):060501, (2011).
- [23] D. CARRALERO et al., On the role of filaments in perpendicular heat transport at the scrape-off layer. *Nucl. Fusion*, **58**(9):096015, (2018).
- [24] S. RIENÄCKER et al., Survey of the edge radial electric field in L-mode TCV plasmas using Doppler backscattering, *Plasma Phys. Control. Fusion* **67** 065003 (2025).
- [25] O. KRUTKIN et al., A method for density fluctuation measurements using pulse reflectometry, *Nucl. Fusion* **63** 076012 (2023).
- [26] Y. H. Xu et al., Investigation of self-organized criticality behavior of edge plasma transport in Torus experiment of technology oriented research, *Physics of Plasmas* **11** (12), (2004).
- [27] J.A. BOEDO et al., Transport by intermittent convection in the boundary of the DIII-D tokamak, *Phys. Plasmas* **8**, 4826–4833, (2001).
- [28] N. OFFEDDU et al., Analysis techniques for blob properties from gas puff imaging data, *Rev. Scient. Instrum.* **94**(3), 033512 (2023).
- [29] S. RIENÄCKER et al., Edge Radial Electric Field in Positive and Negative Triangularity Plasmas in the TCV Tokamak, submitted to *Nucl. Fusion* on 11 Jul 2025.

